Autonomous Component Carrier Selection for 4G Femtocells

A fresh look at an old problem

Garcia, Luis Guilherme Uzeda; Kovacs, Istvan; Pedersen, Klaus; Da Costa, Gustavo Wagner Oliveira; Mogensen, Preben

Published in:
I E E E Journal on Selected Areas in Communications

DOI (link to publication from Publisher):
10.1109/JSAC.2012.120403

Publication date:
2012

Document Version
Early version, also known as pre-print

Autonomous Component Carrier Selection for 4G Femtocells – A fresh look at an old problem –

Luis G. Uzeda Garcia, István Z. Kovács, Klaus I. Pedersen, Gustavo W. O. Costa, and Preben E. Mogensen,

***Abstract*—This paper addresses the interference management problem in the context of LTE-Advanced femtocells. Due to the expected large number of user-deployed cells, centralized network planning becomes increasingly less viable. Consequently, we consider an architecture of autonomous decision makers. Our main contribution in this paper, denominated Generalized Autonomous Component Carrier Selection (G-ACCS), is a distributed carrier-based inter-cell interference coordination scheme that represents one step towards cognitive radio networks. The algorithm relies on expected rather than sensed interference levels. This approach facilitates scheduler-independent decisions, however, it can lead to overestimation of the interference coupling among cells when the resources are not fully utilized. Acknowledging this fact, G-ACCS leverages the power domain to circumvent the restrictive nature of expected interference coupling. This work focuses on the downlink and also provides an extensive characterization of the network performance as a function of the topology as well as the often overlooked temporal traits of traffic. We compare G-ACCS with other carrier-based solutions, including the simplest universal reuse strategy. The encouraging simulation results demonstrate that G-ACCS achieves an efficient and fair distribution of resources in all considered traffic and deployment conditions. More importantly, this is attained in a truly autonomous fashion, without any explicit parametrization.**

***Index Terms*—Femtocells, LTE-Advanced, Carrier Aggregation, Interference Management, Performance Analysis**

I. Introduction

WIRELESS communication networks are essential and ubiquitous elements of modern life, and now small cellular base stations are finding a place in our homes and offices. These devices known as femtocells [1] are expected to play a major role in improving the spectral efficiency per unit area. Yet, the *ad-hoc* nature of femtocell deployments alongside the foreseen closed subscriber groups (CSG) – only a few registered users may be served by the femtocell – is bound to result in chaotic inter-cell interference if resources are allowed to be reused without any restriction. Most ongoing efforts focus on solutions to control the cross-tier (macro-femto) interference in case of co-channel deployments [2]–[5]. However, severe interference among femtocells will be an inevitable reality as future femtocell deployments become denser, similarly to existing WiFi networks [6].

Early considerations in [1], [7] had already suggested that interference avoidance rather than suppression techniques is likely to form the basis of a sensible strategy to ensure high performing uncoordinated local area deployments. Frequency planning was and still is the most traditional approach to guarantee a minimum carrier-to-interference ratio (C/I) at the expense of spectral resources available to cells. At the heart of frequency planning lies the old channel allocation problem, whose essence is deciding how many, which and when channels should be used by each cell in the network.

Channel allocation is a challenging topic that accompanies cellular networks since the concept was introduced by Bell Labs in the 1970s. Not surprisingly, channel assignment algorithms have been extensively investigated and a monumental amount of material is now available in the literature. Although inter-cell interference remains the crux of the matter, many of the original working assumptions have changed dramatically due to recent developments.

A. Recent Developments

We initiate the discussion by outlining a few important paradigm shifts. While some developments challenge our previous understanding of channel allocation techniques, others make a fresh look at the old channel allocation problem very opportune.

For example, LTE – described in [8] – replaces the circuit-switched architecture by an all-IP packet-switched one. In the latter, due to fast statistical multiplexing, channels are shared, and hard blocking plays a much lesser role than in previous channel allocation studies. Furthermore packet bursts are much more ephemeral than voice calls. As a result, fully distributed dynamic resource assignment on a packet or session basis is no easy feat, which is made even harder by inherent signaling delays.

On the other hand, two prominent features of LTE-Advanced [9], [10] are carrier aggregation (CA) [11], [12] and the enhanced support for heterogeneous networks (HetNets) [13]. The former is the agreed method within 3GPP to achieve bandwidths up to 100 MHz, while the latter consists of a conventional cellular network overlaid with one or more micro, pico and/or femtocells. More importantly, CA is a natural enabler of simple, yet effective frequency domain interference management schemes that offer protection to both data and control channels [14]. Furthermore, unlike macro cellular networks, where the careful placement of base stations

alleviates inter-cell interference, most HetNets are particularly subject to heavy inter-cell interference due to the unplanned positioning of cells. Accordingly, HetNets calls for scalable of interference management solutions. A summary of possible solutions considered in 3GPP can be found in [15].

Last, but not least, the vision of cognitive radio networks (CRN) [16] has revamped the academic interest in the distributed version of the channel assignment problem due to its self-organizing nature and its potential to reduce operational expenditures. Given the synergy between HetNets and CA in light of CRN, the fundamental problem discussed in this paper is the design of practical self-adjusting component carrier (CC) selection mechanisms to deal with interference in future LTE-Advanced femtocell deployments.

B. Related Work

Mathematically, channel assignment is a combinatorial optimization problem which can be mapped into a conflict graph vertex (multi-) coloring, hence the problem is often analyzed in light of graph (multi-) coloring [17]–[19]. Although the problem is known to be NP-hard [20], several centralized and distributed coloring algorithms exist. While earlier studies were mostly based on the usage of (generalized) unit disk graphs to model ad-hoc networks [21], recent proposals deal with dense deployments of WLAN networks [22], [23].

An excellent overview and systematic performance comparison of several channel allocation algorithms in the context of circuit-switched networks can be found in [24] and [25], respectively. An insightful theoretical analysis of the stability of distributed dynamic channel allocation technique is presented in [26]. Readers will find a more up-to-date to overview in [27].

With the emergence of decentralized packet switched cellular networks, dynamic spectrum approaches and cooperation are steadily gaining momentum. These solutions typically consider a decentralized architecture of autonomous decision makers. Game Theory studies such interactions and has been applied to dynamic spectrum sharing in a number of recent proposals [28]–[30]. A survey of dynamic spectrum management and cognitive radio (CR) developments is presented in [31]. The coexistence problem between macrocell and femtocell systems is also addressed by means of reinforcement learning techniques in [32], where the authors propose a new docitive paradigm in order to speed up the slow and complex cognitive process. Finally, stochastic geometry and related concepts have also been applied to investigate fully distributed networks consisting of randomly located devices, akin, but not limited to femtocells [33].

One important aspect that most contributions so far fail to consider is the presence of traffic variability. Although optimality and quick convergence may be sufficient from a purely theoretical perspective, these are not the only concerns, stability and robustness (minimal perturbation) are equally, if not more, relevant. In dense deployments, femtocells can (re-)appear at anytime and anywhere, and traffic characteristics often deviate from the idealized full-buffer assumption. Therefore, even if the system converges very quickly, uncontrolled/unpredictable reconfigurations remain a major nuisance and pose several practical problems. Consequently, depending on the application, it might be preferable to exchange optimality for inertia, i.e. resistance to reconfigurations.

C. Paper Overview

This paper presents a systematic evaluation of the effects of inter-cell interference on the overall performance of femtocells through detailed system level simulations. Because the complementary co-channel cross-tier interference is already receiving significant attention in the literature [2]–[5], this contribution concentrates on the inter-cell interference among femtocells operating in a dedicated band, i.e. macro cell and femtocell users are made orthogonal through bandwidth splitting. This is also the simplest way to avoid coverage holes due to the presence CSG femtocells.

Among our contributions, we evaluate and compare four distributed carrier-based interference management solutions. Beginning with the obvious candidate: universal reuse, the techniques are introduced in increasing order of complexity. The ultimate goal is to identify the trade-offs and assess how much complexity is effectively required to provide efficient interference coordination on a CC level in the context of LTE-Advanced femtocells.

The rest of the paper is organized as follows: Section II formulates the problem and sets the scene with the help of an insightful numerical example. The latter is also used throughout the paper to complement the observed results via intuitive explanations. The considered solutions are described in Section III. Most notably, we propose a novel and decentralized "cognitive" solution that enables femtocells to jointly determine the subset of CCs and their corresponding transmission power levels, such that existing transmissions from neighboring cells are not disrupted. Section IV introduces our working assumptions, while Section V presents an extensive comparative analysis of the considered alternatives. We focus on the downlink and heed the often overlooked case of time-varying interference due to random session arrivals and finite payloads. The analysis encompasses the effects of spatial density (network topology) and temporal sparseness (activity factor) on network performance. To the best of our knowledge, a comprehensive evaluation of these two aspects is not available in the context of interference coordination schemes for femtocells. Finally, Section VI recapitulates the main findings and concludes the paper.

II. System Model and Problem Formulation

We define a network as a set of N femtocells, denoted by $\mathcal{N} = \{1, \ldots, N\}$ operating in a licensed band of $\mathcal{B}$ MHz. The spectrum is divided into a set $\mathcal{C}$ of component carriers of cardinality $|\mathcal{C}| = C$. Without loss of generality, we assume that $BW(c) = \mathcal{B}/C \ \forall \ c \in \mathcal{C}$ and that all CCs experience approximately the same propagation conditions. Nonetheless, the interference footprint of each CC can be substantially different due to mobility and time-varying load conditions.

The problem at hand is to find the subset $\Lambda(n) \subseteq \mathcal{C}$ of CCs that each cell n should deploy given the topology of the network and its current traffic conditions. We pay special

attention to the nuances of interference footprint in local area deployments and do not address the case of co-channel interference to/from macrocells in overlaid networks.

In order to avoid confusion, we also highlight that the proposed selection of CCs is femtocell-specific, which differs from the UE-specific CC assignment. As explained in [12], the latter implies that the set of CCs a base-station (eNB) is allowed to use is pre-determined, but UEs can be configured independently. Each served UE must be provided with a single primary serving CC – denoted *Pcell* – and possibly one or more additional serving CCs, called secondary serving cells (*SCells*) depending on its quality of service (QoS) requirements.

The basic principle of femtocell-specific CC is the division of CCs into two categories: base and supplementary. The former is the main component carrier to be used by femtocells. The main CC acts as an anchor and has full cell coverage. Although this main CC has been previously referred to as the primary component carrier (PCC) in [14], henceforth, we shall denote it as base component carrier (BCC) in order to avoid confusion with the UE-specific CC terminology. Any additional cell-specific CCs (beyond the BCC) will be referred to as supplementary component carriers (SCCs) and are chosen upon demand.

A. Preliminaries: The Background Interference Matrix

Given that the numerical example in this section and two of the proposed methods in Section III rely on Background Interference Matrices (BIMs), we discuss them separately building upon the work in [14]. Readers familiar with the concept may proceed to the next section heeding the notation introduced by (1) and (2).

BIMs are built via a combination of local and exchanged pieces of information based exclusively on downlink measurements. The local information essentially predicts the *potential* DL (incoming) C/I experienced by the served UEs; realized when the given pair of cells (serving and interferer) use the same CC at the same time with equal transmit power spectral densities (PSDs). Similarly, the exchanged information makes cells aware of their individual contributions as *potential* sources of (outgoing) interference. Without loss of generality and solely in order to preserve light notation, we assume that each femtocell has knowledge of the other $N-1$ cells in the network, understanding that the predicted C/I ratio can be set at an arbitrary high value for all distant and undetectable neighbors. The latter indicates the lack of interference coupling between these cells. Notwithstanding, a practical implementation does not necessitate global knowledge.

Each active UE, m, connected to a cell performs measurements of reference signal received power (RSRP) [34] levels which are reported to its serving cell. These measurements conducted both towards the serving and surrounding cells do not represent an extra burden on the UE side, because such measurements are performed regularly for e.g. handover purposes. In possession of these measurement reports, each femtocell, k, then builds a local $M \times N$ matrix $\mathbf{\Gamma}^k$, where M is the number of UEs served by femtocell k, and N is the number of femtocells in the network. Each γ^k_{mn} entry is given by the ratio:

$$\gamma^k_{mn} = \begin{cases} \dfrac{G_{\{m\}\leftarrow\{n\}}\rho_k}{\eta} & n = k \\ \dfrac{G_{\{m\}\leftarrow\{k\}}}{G_{\{m\}\leftarrow\{n\}}} & \text{otherwise.} \end{cases}$$

Above, $G_{\{x\}\leftarrow\{y\}}$ reflects the composite channel gain (averaging out fast-fading) between user x and femtocell y. The channel gains can be readily estimated by femtocell k based on the information fed back by UE m, because the transmission power of reference symbols ρ_k is known a priori (the same in all cells or alternatively signaled between cells). Here, η is the thermal noise power assumed the same for all users.

In order to curb the control signaling overhead, the assumption in [14] is that this local information is first "fused" before being exchanged. Due to the very limited number of users served by femtocells, the proposed data fusion process is rather simple[1]. The $M \times N$ matrix is compressed into a $N \times 1$ (incoming) column vector $\mathbf{i}^k = \begin{bmatrix} i^k_1 & i^k_2 & \dots & i^k_N \end{bmatrix}^T$ such that $i^k_n \triangleq \min(\gamma^k_{*n})$, i.e. each element is taken as the minimum value of the corresponding column of $\mathbf{\Gamma}^k$. Conceptually, this implies that measurements from the UE that would experience the lowest C/I ratio in case of simultaneous usage of a given CC dictate the values that are effectively exchanged. Once mutual information exchange takes place between all pairs of cells – each cell sending and receiving a single quantized value to/from its peer – a second $N \times 1$ (outgoing) column vector $\mathbf{o}^k = \begin{bmatrix} o^k_1 & o^k_2 & \dots & o^k_N \end{bmatrix}^T$ such that $o^k_n \triangleq i^n_k$ becomes available. Finally the $N \times 2$ BIM of cell k is then:

$$\text{BIM}_k = \begin{bmatrix} \mathbf{i}^k & \mathbf{o}^k \end{bmatrix} \tag{1}$$

In the remainder of this paper, we shall denote the DL incoming and outgoing interference couplings as $DL_{\{.\}\leftarrow\{.\}}$ and $DL_{\{.\}\rightarrow\{.\}}$, respectively. Note that for any given pair $\langle k, n \rangle$ of cells the following holds:

$$\begin{aligned} DL_{\{k\}\leftarrow\{n\}} &\equiv \text{BIM}_k(n,1) \\ &\equiv \text{BIM}_n(k,2) \\ &\equiv DL_{\{n\}\rightarrow\{k\}} \end{aligned} \tag{2}$$

B. Numerical Example

We now introduce a simple numerical analysis which will be used throughout the paper to provide intuitive explanations. The basic scenario is shown in Fig. 1. It consists of 2 CSG femtocells $\{A, B\}$, each cell serving a single UE, $\{\alpha, \beta\}$, respectively. For simplicity, we assume that both cells share a single (spectral) resource – e.g. a component carrier – each with a (temporal) activity factor denoted by $0 < P_x \leq 1, x \in \{A, B\}$. Although both cells have at least in principle equal rights to use the spectral resources, highly asymmetrical (unfair) situations may arise due to the uncoordinated nature of femtocell deployments. We begin by quantifying in (3)-(4) the value of selfishness relative to perfect cooperation

[1]The same framework can be extended to the context of pico and even macrocells. However, the data fusion process should be adapted.

(ideal interference avoidance) as perceived by cells A and B, respectively.

$$\Xi_A \triangleq \frac{P_A P_B\, \varepsilon_A\, \mathrm{C_{MAX}} + P_A(1-P_B)\, \mathrm{C_{MAX}}}{\min\{P_A; \max[(1-P_B); 0.5]\}\, \mathrm{C_{MAX}}} \quad (3)$$

$$\Xi_B \triangleq \frac{P_B P_A\, \varepsilon_B\, \mathrm{C_{MAX}} + P_B(1-P_A)\, \mathrm{C_{MAX}}}{\min\{P_B; \max[(1-P_A); 0.5]\}\, \mathrm{C_{MAX}}} \quad (4)$$

Our equations can be interpreted as follows: the numerators in (3)-(4) estimate the attained DL throughput in the absence of coordination. As such, P_A and P_B act as independent transmission probabilities. The resulting throughput of cell x is then given by a weighted sum. $\mathrm{C_{MAX}}$ – the highest achievable throughput due to modulation and coding scheme (MCS) limitations – is achieved when there is no collision. Logically, in case of simultaneous transmissions, cell x attains only a topology dependent fraction, ε_x, of it.

On the other hand, the denominators quantify the achieved DL throughput when transmissions are always forced to be orthogonal. In this case, each cell cannot have an activity factor higher than 50% in general. The exception being the case where one cell's activity can be fully or at least partially accommodated due to modest resource needs of its neighboring cell, i.e. an ideal white-space filling strategy is assumed.

In summary, ratios higher than one imply that a cell benefits from no coordination whatsoever. Conversely, ratios smaller than one signify that the cell would favor a cooperative (orthogonal) approach even if that means capping its activity. Now, coming back to Fig. 1 and observing the existing asymmetry coupled with the CSG premise, we assume the following: $\mathrm{DL}_{\{A\}\leftarrow\{B\}} = G_{\{\alpha\}\leftarrow\{A\}}/G_{\{\alpha\}\leftarrow\{B\}} = 20\mathrm{dB}$ and $\mathrm{DL}_{\{B\}\leftarrow\{A\}} = G_{\{\beta\}\leftarrow\{B\}}/G_{\{\beta\}\leftarrow\{A\}} = -5\mathrm{dB}$. Thus, numerically:

$$\varepsilon_A \triangleq C_{A|B}/\mathrm{C_{MAX}} \approx 0.74 : C_{A|B} = \mathcal{S}\left(\mathrm{DL}_{\{A\}\leftarrow\{B\}}\right)$$

$$\varepsilon_B \triangleq C_{B|A}/\mathrm{C_{MAX}} \approx 0.06 : C_{B|A} = \mathcal{S}\left(\mathrm{DL}_{\{B\}\leftarrow\{A\}}\right)$$

Here $\mathcal{S}(.)$ is a function that maps C/I into spectral efficiency and $C_{X|Y}$ denotes the throughput achieved by cell X when cells X and Y have colliding transmissions. In our example, $\mathcal{S}(.)$ is an adjusted Shannon formula proposed in [35] for LTE. The curve fitting parameters were taken from tables 3 and 4 of the same paper. Nonetheless, the evaluation remains equally valid if the theoretical bounds for channel capacity [36] are used. The only three constraints are:

- Thermal noise is negligible and inter-cell interference is treated as noise by receivers.
- Below a minimal Signal-to-Interference-plus-Noise (SINR), the achieved throughput is zero because UEs are not even able to synchronize with their serving cells.
- Due to practical MCS limitations, the achievable throughput does not increase indefinitely with SINR.

The outcome is shown in Figs. 2a and 2b as a function of the activity factors P_A and P_B. The color indicates the value of $(\Xi_x - 1)\cdot 100$. The line segments in Figs. 2a and 2b demarcate the convex hull of the region where nodes have a strict preference for selfish behavior. Fig. 2a shows that cell A has

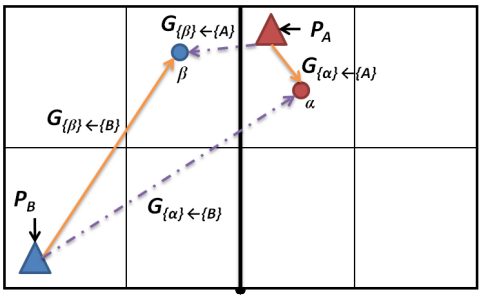

Fig. 1. An example of a highly asymmetrical deployment of two CSG femtocells. The solid and dashed lines represent signal and interference channel gains respectively. Circles represent UEs, while triangles the femtocells.

a weak predisposition for cooperation when its activity is low. However, when P_A goes beyond 60%, the inclination towards selfishness is extremely strong. The achievable throughput due to selfish behavior is nearly twice as high as that attained by cooperating. Conversely Fig. 2b depicts that cell B strongly favors cooperation with the exception of a minuscule region where its activity ratio is nearly 100%, and cell A is rather inactive. Nonetheless, if cell A decides to seek its own benefit, cell B is virtually helpless and loses nearly all of its capacity as the numerator in (4) approaches zero in a very wide area of Fig. 2b. Briefly, Fig. 2 conveys two important messages:

- Selfish approaches might be optimal if sum-capacity is the metric of interest; notwithstanding, if fairness and outage-capacity are to be taken into account, cells – especially CSG ones – need to mind their surroundings.
- Network topology essentially governs the interaction of cells, yet the activity patterns affect the perception cells have of their environment.

III. Autonomous Component Carrier Selection Strategies

In this section, we recur to the problem at hand and identify some strategies to tackle it. While in theory, algorithms should strive for optimality, in practice, cells should avoid frequent and abrupt reconfigurations. For example, the reselection of the entire set of CCs by any given cell, implies resetting that cell, which in turn leads to undesirable service interruptions.

For this reason, all investigated algorithms are essentially non-iterative and operate on time scales much longer than that of scheduling decisions. In fact, such algorithms embody a new RRM entity, which deals solely with the CC acquisition rules whenever the need is raised by the independent packet schedulers. This is the preferred approach because it is nearly impossible to get different vendors to agree upon cooperation rules built into their proprietary packet schedulers. Therefore, schedulers are free to distribute the resources of the selected CCs among its UEs according to any internal metric. One way to achieve this scheduling independence is to rely on the estimation of potential interference coupling as in BIMs, rather than actual interference temperature measurements. Such approach, albeit suboptimal, has two important advantages:

- Interoperability among vendors.
- Independence from scheduling decisions.

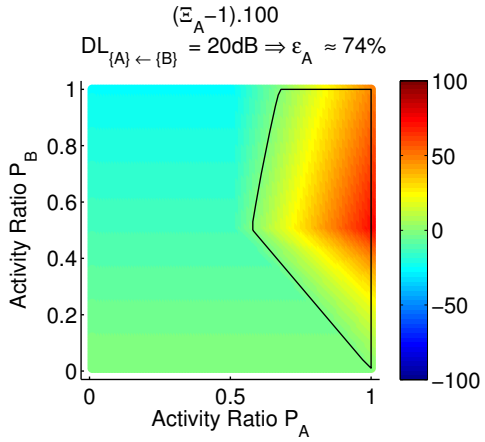

(a)

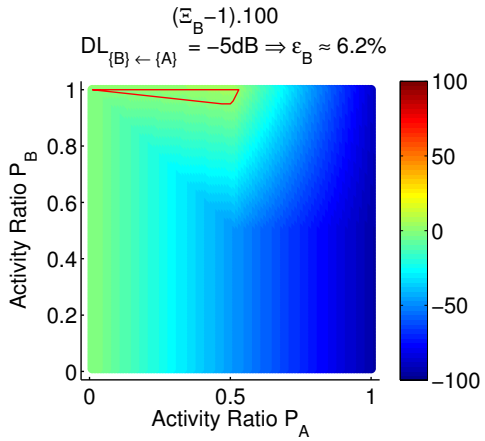

(b)

Fig. 2. Relative value of selfishness with respect to perfect cooperation aiming at orthogonal transmissions: (a) $(\Xi_A - 1) \cdot 100$ and (b) $(\Xi_B - 1) \cdot 100$.

While the advantage of interoperability is unequivocal, the benefit of independence from (distributed) scheduling decisions might not be straightforward, but it is deep-rooted in the time-varying nature of the problem. Because traffic demand varies (on several time-scales), methods that rely purely on actual interference temperature, rather than potential interference, have to deal with two grave practical issues: (i) tracking a rapid moving target – signal and interference vary due to scheduling, power, channel and traffic conditions – and (ii) adjusting the resources accordingly. However, by doing so, they modify the interference footprint, which mandates an iterative process and can, in a worst-case scenario, lead to a causality dilemma. This serious convergence issue is often downplayed, since most studies normally assume very stable interference conditions due to the underlying, yet unrealistic, full-buffer traffic assumption.

We now introduce the four component carrier selection strategies considered in this paper. All of which purposefully avoid the foregoing convergence and stability issues at the expense of optimality. Henceforth, we assume that the system bandwidth consists of 5 CCs, the maximum supported by LTE-Advanced [11].

A. Universal Reuse

Although not strictly a CC selection strategy, there is no simpler approach than to grant all femtocells unrestricted access to all 5 CCs at all times without any power restrictions. Early work [37] based on LTE macro-cells indicate that among the static frequency schemes, plain reuse 1 performs best for wideband services. On the other hand, findings in [38] suggest that a properly chosen reuse factor leads to significant gains in 5%-outage user throughput in uncoordinated local area deployments. However, both studies assume full-buffer traffic. For this reason and also due to its inherent simplicity, we include universal reuse in our evaluation. Referring to Fig. 2 in Section II-B, reuse 1 is a simple strategy whose overall performance strongly depends on favorable network topology and activity ratios.

B. Network Listening Mode

A second possibility is to make use of the sensing capabilities of femtocells. Based on findings in [38] where a reuse factor of $1/2$ showed promising results, we employ a pragmatic approach where the 5 CCs are split into two semi-orthogonal subsets $\Lambda_1 = \{1, 2, 3\}$ and $\Lambda_2 = \{3, 4, 5\}$. During startup, each femtocells enters into a Network Listening Mode (NLM) [39] phase. Acting as a pseudo-UE, the femtocell scans the air interface searching for DL pilot signals from other femtocells in order to select the complementary subset to the one utilized by its "nearest" neighbor, i.e. the one with the smallest estimated path loss. The selected subset is not changed afterwards, at least not in a short time span, recognizing that the outcome cannot be expected to be the best possible. As opposed to universal reuse this approach clearly leverages the network topology and can partially avoid interference. Once again looking at Fig. 2 and considering just one cell and its "nearest" neighbor, this solution can be understood as a hybrid one. Both cells attain orthogonal allocations for two CCs and share a third one where the outcome will again depend on the traffic intensity.

C. Basic ACCS

In this paper we build upon the work originally presented in [14], [40]. In those papers, we proposed a fully distributed and slowly-adaptive concept known as autonomous component carrier selection (ACCS). The method was described in detail in the aforementioned references. Therefore, we restrict ourselves to a brief description of the fundamental aspects highlighting important developments not described previously.

As described in Section II, component carrier are divided into two cell-specific categories: base (BCC) and supplementary (SCC). The former is the main CC to be used by femtocells. The latter denotes additional CCs deployed upon demand. Unused CCs are totally muted, including control channels. ACCS employs the information stored in the BIM (Section II-A) as well as knowledge of the CC usage of neighboring cells to figure out whether or not a new SCC allocation will jeopardize any existing allocation based on target C/I values. ACCS also assumes a priori knowledge of

the configurable C/I targets (thresholds) for both BCC and SCCs.

Here, we propose two minor changes: First, we suggest the usage of a separate and much lower C/I target for the incoming interference estimation. The original concept treated incoming and outgoing estimations equally. By doing so, it failed to recognize that from a cell-centric perspective more bandwidth is never harmful as long as the expected incoming C/I is still above the lower bound imposed by MCS limitations. The outgoing evaluation remains the same. Another important aspect is the decoupling between DL and UL decisions due to the potentially asymmetrical traffic requirements. Decoupled decisions have little impact on the DL, since ACCS is chiefly based on DL information. Additionally, the studies in [41] show that UL performance is not compromised either.

A parallel can also be drawn between the basic ACCS and the discussion in Section II-B. First, similarly to the NLM approach, ACCS gathers information related to the network topology. Notwithstanding, this information – the BIM – characterizes the receiving UE conditions and not those of the transmitting femtocell. Moreover, when it comes to allowing non-orthogonal transmissions, ACCS distinguishes between both cells. For example, if cell B in Fig. 1 is using a certain CC, and cell A decides to deploy it as well, the allocation will be denied in order to ensure minimal disturbance of ongoing transmissions. The opposite, however, would be allowed since cell B would not seriously harm UE α.

D. Generalized ACCS (G-ACCS)

1) Problem delineation: In the basic ACCS concept discussed previously each CC is eligible for use in any cell provided that certain parameterized C/I requirements are satisfied. However, the C/I constraints, to which cells are required to adhere during SCC selection, may act as an over-protective limitation, especially when the rapid varying nature of packet switched traffic is considered. Unless the CC is fully utilized ($P_A = P_B = 100\%$ in our model from Section II-B) capacity that could otherwise be utilized is actually wasted because interference is overestimated. In fact, moving from a pairwise interference coupling characterization towards a "global" one as suggested in [42], where contributions from/to all cells are aggregated, would aggravate the overestimation problem even further.

2) Proposed Solution: In this section we extend the original idea to deal effectively with the time-domain related aspects of CC selection. The objective is to render the distribution of SCC less sensitive to the temporal evolution of the bandwidth acquisition/waiver process. In summary, we propose the proactive usage of the information found in the BIMs to set the power spectral density (PSD) of a desired CC autonomously. The goal is to provide a balance between the minimization of the outgoing interference and the usefulness of a given CC. Moreover, it should be appreciated that whilst our description is primarily in relation to the DL situation, the same scheme can also be employed in the UL.

The proposed scheme retains the first-come first choice service policy of ACCS but allows cells selecting their CCs later on to try and allocate new CCs provided that these cells reduce their PSD in order to minimize the outgoing interference towards the cell currently holding that CC. The cell which currently holds a particular CC is referred to as a *prior cell*. The cell which tries to deploy the same CC later on is denominated a *posterior cell*. In cognitive radio jargon [16], the prior femtocell acts as the primary device, while the posterior femtocell plays the role of a cognitive secondary radio. The method attempts to maximize the capacity of both posterior and prior cells under two restrictions:

(a) Prior cells have higher priority and shall never incur capacity losses larger than the potential capacity gain attained by posterior cells.
(b) Posterior cells are the only cells performing power reductions. The PSD of prior cells remains unchanged and posterior cells utilize this assumption.

These two restrictions provide the mathematical framework under which the ideal PSD is calculated autonomously by posterior cells during the CC allocation attempt. This is on the basis that if the prior cell has very little or nothing to lose, the posterior cells should allocate the CC, even if the yield to the posterior cell is low due to incoming interference. Conversely, if the prior cell is estimated to experience a critical capacity loss due to outgoing interference, the posterior cell refrains from allocating the desired CC irrespective of its potential capacity gain. It is also important to notice that such denominations are not absolute. After playing the role of a posterior cell when trying to deploy CC c, the same femtocell might be regarded as a prior by another cell attempting to enable the same CC subsequently.

Besides the BIM, another central pillar of G-ACCS is the so-called component carrier radio allocation table (CCRAT). The latter consists of pieces of information aggregated by each femtocell via signaling expressing which CCs are currently in use. Along the lines of the discussion in Section II-A and without loss of generality we can model it as a $N \times C$ matrix $\boldsymbol{\Psi} = \begin{bmatrix} \boldsymbol{\psi}_1 & \boldsymbol{\psi}_2 & \dots & \boldsymbol{\psi}_C \end{bmatrix}$ where each $N \times 1$ vector $\boldsymbol{\psi}_c$ informs the usage of component carrier c by the N cells in network and their respective (if any) PSD *reduction*. The n^{th} entry of $\boldsymbol{\psi}_c$ according to the CC usage is such that:

$$[\boldsymbol{\psi}_c]_n = \begin{cases} z_n^c & \text{c is used by cell n.} \\ \infty & \text{c is unused by cell n.} \end{cases}$$

Where z_n^c represents the PSD reduction (relative to a common maximum PSD) applied by cell n to CC c. Notice that unused CCs are completely muted, hence the infinite PSD reduction. Once cell k detects the need for additional CCs, it will use the information found in the BIM and CCRAT to figure out whether or not the new allocation will jeopardize any existing allocation. Recap that the BIM values are C/I estimates assuming equal power levels. Therefore, the PSD reductions of both the prior and posterior cell have to be taken into account on the C/I estimates.

G-ACCS exchanges the capacity yield of the posterior cell for the loss of the prior cell in order to make an allocation decision. The selected transmit power for each CC maximizes the difference of the yield and the loss, i.e., the net yield.

The subsequent capacity estimation, i.e. mapping C/I into spectral efficiency, relies on the function $S(.)$ as explained in Section II-B.

The loss of the most critical prior cell, ω, is calculated as:

$$l(x) = S_{\text{free}} - \mathcal{S}\left(\text{DL}_{\{k\}\rightarrow\{\omega\}} - z^c_\omega + x\right) \tag{5}$$

where S_{free} represents the current capacity of the prior cell ω as discussed later in this section, x is the power reduction of the posterior cell, and z^c_ω is the power reduction of the prior cell ω in dB[2]. The evaluation is done for each desired CC, c. Note that the argument of $S(.)$ in (5) is an effective outgoing BIM C/I as corrected by the PSD reductions. The most critical prior cell, ω, is determined for each CC as follows.

Denoting the set of neighboring prior femtocells currently using the candidate CC as $\boldsymbol{\psi}_{c\setminus\infty}$ ($\boldsymbol{\psi}_c$ excluding non-finite entries); then cell ω in (5) is such that:

$$\omega \triangleq n \mid \forall m \in \boldsymbol{\psi}_{c\setminus\infty} : \text{DL}_{\{k\}\rightarrow\{n\}} - z^c_n \leq \text{DL}_{\{k\}\rightarrow\{m\}} - z^c_m$$

i.e. it corresponds to the prior cell with the lowest effective outgoing BIM C/I entry – accounting for eventual PSD reductions – amongst all those currently using the desired CC as seen in the CCRAT table. In other words, the most affected prior cell in the case that the posterior cell uses the component carrier as well.

Similarly, the yield is defined in terms of the lowest effective incoming BIM C/I; PSD reduction included:

$$y(x) = \mathcal{S}\left(\text{DL}_{\{k\}\leftarrow\{\iota\}} + z^c_\iota - x\right) \tag{6}$$

where ι in (6) is defined to be the neighboring cell from $\boldsymbol{\psi}_{c\setminus\infty}$ responsible for the lowest effective incoming BIM C/I entry amongst all those currently using the desired CC as seen in the CCRAT table. It should be appreciated that such a cell is not necessarily the prior cell ω considered in (5) given a possible asymmetry of the interference coupling. Therefore:

$$\iota \triangleq n \mid \forall m \in \boldsymbol{\psi}_{c\setminus\infty} : \text{DL}_{\{k\}\leftarrow\{n\}} + z^c_n \leq \text{DL}_{\{k\}\leftarrow\{m\}} + z^c_m.$$

Finally, the net yield $n(x)$ is simply the difference of the yield $y(x)$ and the loss $l(x)$:

$$n(x) = y(x) - l(x) \tag{7}$$

G-ACCS analyzes what is a possible power reduction x that maximizes the net yield. After analyzing $n(x)$ in (7); the CC will be deployed by the posterior cell if and only if:

$$\exists\, x \in [0 \quad \varrho] : n(x) \in \mathbb{R}^+ \tag{8}$$

where ϱ denotes the maximum applicable PSD reduction. In this case, x is set at $\hat{x}$ given by:

$$\hat{x} = \underset{x\in[0\ \varrho]}{\arg\max}\ n(x) \tag{9}$$

Naturally, if $\boldsymbol{\psi}_{c\setminus\infty} = \emptyset$, the CC can be taken without any further considerations.

In a basic implementation, the constant S_{free}, in (5), corresponds to the maximum spectral efficiency achievable by the system, i.e. the bandwidth of the CC is interference free. Optionally and more realistically, S_{free} could correspond to an estimation based on the average experienced SNR or even SINR at the prior cell just before the allocation attempt. Nevertheless these two alternatives entail additional signaling in order to inform the posterior cell about the conditions in the prior cell. For this reason, the first approach is preferred.

Algorithm 1 summarizes the proposed method. We resort to iterative numerical optimization because the function $n(x)$ is not differentiable. This is not a limitation of the framework itself, it is rather a consequence of $S(.)$ trying to mimic the behavior of a real system.

Algorithm 1 Calculate the PSD reduction $\hat{x}$

```
for each desired CC do
  Identify cell ω
  Identify cell ι
  if ∄ cell ω then
    Allocate ← true {CC is free.}
    x̂ ← 0
  else
    x̂ ← ∞, x ← 0, N_max ← 0
    while x ≤ ϱ do
      Increase x
      Estimate n(x)
      if N_max < n(x) then
        N_max ← n(x)
        x̂ ← x
      end if
    end while
    Allocate ← N_max ≠ 0
  end if
  return Allocate, x̂
end for
```

IV. Performance Evaluation

A. Simulation Tool

The performance was evaluated in a quasi-dynamic system level simulator. The basic LTE physical layer specifications [43] is the basis for the simulator. In addition to that, the simulation tool supports carrier aggregation and the dynamic selection of CCs. The statistical reliability of the simulation is ensured by collecting the results of thousands of snapshots. Each snapshot lasting over one hundred seconds. During each snapshot, path loss, shadowing and the location of devices remain constant. Fast fading is not explicitly simulated.

Whereas the location of devices is static, RRM and the generation of traffic are dynamic processes. The simple finite-buffer traffic model is aligned with 3GPP recommendations [44] to facilitate independent validations. The model is based on sessions with fixed payloads. The interval $\mathcal{I}$ between the end of one session and the user's request for the next session obeys a negative exponential distribution, with an average length of $1/\lambda$, where λ is the rate parameter.

The packet scheduling algorithm is a simple equal resource sharing (round-robin) scheduler. The DL signal to interference

[2]In (5)-(6) the arguments of $S(.)$ are assumed to have been converted to dB; hence the additions/subtractions.

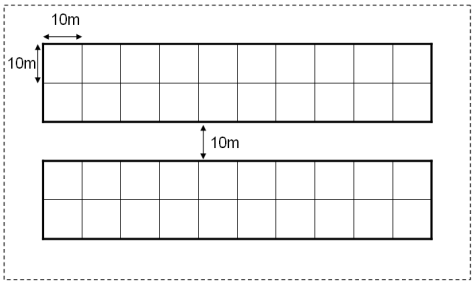

Fig. 3. Top view of the deployment scenario. Three floors are used.

and noise ratio (SINR) is calculated per physical resource block (PRB) for every simulation step. Error vector magnitude (EVM) modeling is included; therefore SINR is asymptotically limited. Finally, in order to calculate the achieved throughput, we apply a modified Shannon fitting. In our simulations as well as in our numerical evaluations in Section II-B we employ the parameters found in tables 3 and 4 from [35]. The following 2 modes are considered: single-stream (CLM1) and multi-stream (SM MIMO).

B. Deployment Scenario

The simulation scenario and indoor path loss modeling follow that defined in [44] for the evaluation of femtocells. The scenario consists of two buildings, each with two stripes of apartments, each stripe having 10 apartments per floor in a total of 3 floors, thus totaling 120 apartments. There is a 10m wide street between the two buildings. The scenario is illustrated in Fig. 3. A single femtocell and all its served user(s) are located inside the same apartment under CSG access mode. Their locations within each apartment are random and uniformly distributed. Macro-cells are not considered in this study, or equivalently macro and femtocells operate in separate frequency bands.

C. Simulation Assumptions

Five CCs of 20 MHz are assumed. Although such spectral availability seems optimistic for today's operators, it is not critical. In fact, all results are normalized and therefore independent from the system bandwidth. The number of CCs available is a much more relevant aspect [40]. The total power is distributed evenly among CCs. The fixed payload size is $S = 62.5$ Mbytes[3] and the number of users per femtocell was set at $U = 1$. We study two different scenarios: the first assumes a deployment ratio $\delta = 20\%$ while $\delta = 80\%$ in the second and even denser scenario. Additionally, for each scenario the arrival rate λ parameter took on the following values [0.1 0.2 1]. Each run consisted of 2000 snapshots, each snapshot comprising 120s.

Moreover, since ACCS and G-ACCS rely on information exchange among femtocells, we include a latency of 100 ms in order to account for signaling delays. Therefore if two or more cells attempt to allocate SCCs within a time-window of 100 ms the information will not be available in the CCRAT and a "collision" may occur. Although there are practical ways to deal with this problem, such solutions are beyond the scope of this work. Therefore, the results herein already include imperfections. Another design choice is that in G-ACCS multiple iterations are not allowed. For this reason $\hat{x}$ is calculated only once for the sake of (i) simplicity, (ii) stability and (iii) minimal signaling requirements.

[3]The artificial file size is due to the available bandwidth of 100 MHz. Our goal is to exercise a wide range of workloads (from modest to near full-buffer traffic loads.) One could down-scale file sizes to the desired bandwidth.

TABLE I
ASSUMPTIONS FOR SYSTEM-LEVEL SIMULATIONS

System Model		
eNB parameters	Total TX power	20 dBm
	Tx Power/CC	$[0 \sim 13]$ dBm
Spectrum allocation	5 CCs of 20 MHz each	
C/I thresholds (ACCS)	BCC:15 dB	SCC: 8 dB
Information exchange latency	100 ms	
Total EVM	5%	
Propagation Model [44]		
Shadowing std. deviation	Serving Cell	4 dB
	Other Cells	8 dB
Minimum coupling loss	45 dB	
Deployment and Traffic Models [44]		
Deployment ratios	$\delta = 20\%$ and $\delta = 80\%$	
Inter-session intervals	$E[\mathcal{I}] = 1/\lambda = [10\ 5\ 1]$ s	
Payload Size	62.5 MBytes	

The numerical results were obtained as follows. In each snapshot, the deployed femtocells were activated; one at a time in a random sequence. When universal reuse is employed, all cells may use all 5 CCs, and there are no further considerations. In the NLM simulations, upon activation each femtocell selects one subset based on the preceding network state, and no further changes take place. In (G-)ACCS simulations a single base component carrier (BCC) is selected as in [14] and is not changed afterwards. The process relies on previous decisions made by other femtocells and without any UE-side information. In the subsequent phase of (G-)ACCS simulations femtocells always attempt to select as many SCCs as possible whenever a download session starts, relinquishing them upon completion. This means that the underlying packet schedulers are inherently greedy, but do not occupy extra resources when there is no traffic at all. Yet, the BCC is always kept. There are no additional rules in order not to violate the scheduler independence principle. In all cases, the collection of results begins once all deployed femtocells have been switched on. Finally, Table I provides an overview of the main simulation parameters.

V. Simulation Results and Analysis

All user perceived throughput figures are calculated during active periods. A user is considered to be active from the moment the first packet of a session arrives until the reception of the last packet of the session. Additionally, all throughput results presented next are normalized by the maximum theoretical capacity of the system. Hence, a normalized throughput of 100% implies a transmission over the whole bandwidth at the maximum system spectral efficiency. This emphasizes the relative trends rather than the absolute values. Finally, the key performance indicators used for the evaluation are:

- Average duty cycle (D): it is the fraction of time that the system has active transmissions. Calculated as the ratio of the average duration of downloads $E[\tau]$ and the average total interval between sessions $E[\mathcal{I}+\tau]$.
- G-factor: defined as the ratio of the total wideband signal power and the interference plus noise power at the receiver (UE) side.
- Average cell throughput: the cell throughput averaged over all active cell from all simulation snapshots.
- Peak user throughput: the achieved user throughput for the 95%-tile, i.e. the 5% best users achieve higher (if MCS allows) or at least equal throughput values.
- Outage user throughput: the achieved user throughput for the 5%-tile, the 5% worst users achieve equal or lower throughput values.

A. Topology, Traffic Variability and Network Performance

In this section, we examine the statistical impact of the topology (density) and traffic variability on the overall network performance. The average duty cycle for all evaluated methods and both deployment ratios is plotted in Fig. 4a. Although all methods achieve a similar average duty cycle, G-ACCS shows a consistently lower one in all scenarios considered. The simpler NLM approach suffers from poor performance, especially at sparse deployments – solid magenta line – because it imposes a hard limit on the amount of allocated resources. Such limitation is only efficient when the duty cycle is very high. Two additional aspects can be observed in Fig. 4b which depicts the G-factor distributions for the simplest universal reuse strategy:

- Despite comparable average duty cycles (D=24% and D=19%) the share of users experiencing low G-factor e.g. below 0 dB jumps from 8% to nearly 20% in the denser deployment.
- When $\delta = 0.2$ even the highest loaded system at D=67% (uppermost red solid curve) presents higher G-factor values than the lowest loaded system for $\delta = 0.8$ at D=19% (lowermost dashed blue curve).

These two findings fall in with the discussion in Section II-B and indicate that the density of the network plays indeed a more important role than the traffic intensity in dictating the interaction of cells. Moreover, depending on the traffic intensity universal reuse might be an efficient solution in terms of average performance, but certainly is not a fair one, especially in dense femtocell deployments. In fact, some users will simply starve due to extremely low G-factor conditions.

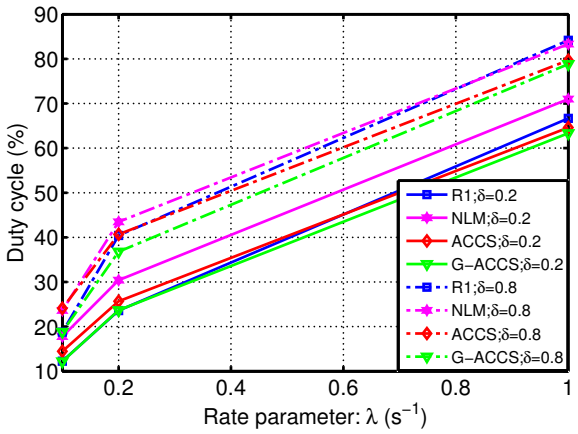

(a)

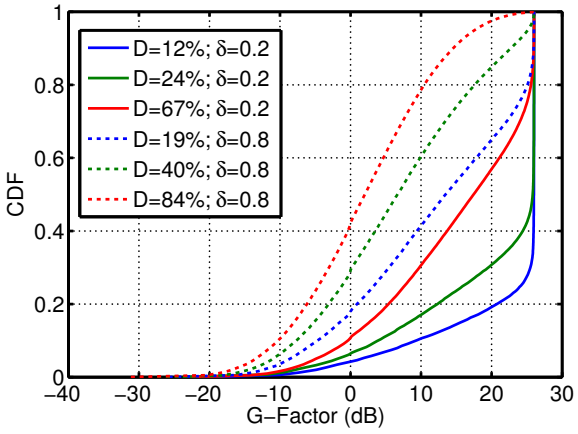

(b)

Fig. 4. (a) Average duty cycle comparison as a function of λ for all evaluated methods and deployment ratios. (b) Empirical G-factor distributions for variable deployment ratios and duty cycles assuming universal reuse.

B. The Downside of Conditional C/I Ratios

The foregoing discussions in Section III highlighted the advantages of utilizing the expected interference coupling between cells rather than actual interference levels. The considerations in Section III-D hinted at the potential pitfalls. Now we examine the subject more carefully. Figs. 5a and 5b depict the empirical cumulative distributions functions of normalized DL cell throughput for $\langle \delta = 0.2, \lambda = 0.1 \rangle$ and $\langle \delta = 0.8, \lambda = 0.1 \rangle$, respectively. For the sake of completeness we also include performance results for the original ACCS scheme presented in [14].

Due to the light traffic load, the interference levels incurred are not necessarily detrimental, hence the superior performance of universal reuse. The overprotection effect of ACCS becomes evident. This arises because BIMs are oblivious to the actual activity ratio of both cells, i.e. all interference coupling estimations correspond to the upper-right corner of Figs. 2a and 2b. Putting more emphasis on the outgoing BIM entries as suggested in Section III-C, rather than treating incoming and outgoing entries equally [14], alleviates the problem. However, the effect is not significant, notably when $\delta = 0.8$. This occurs mainly because many CCs are taken anyway by neighbors as BCCs, which have much stricter C/I targets.

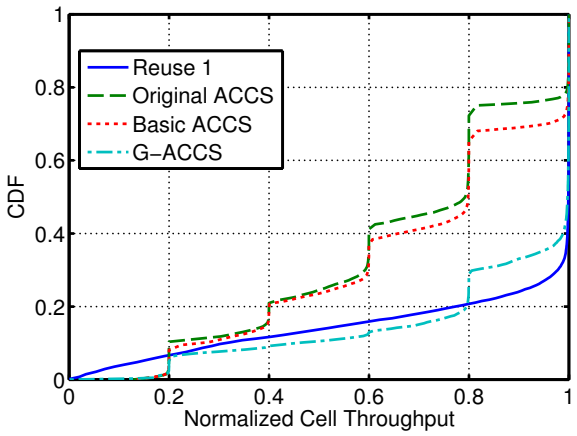

(a)

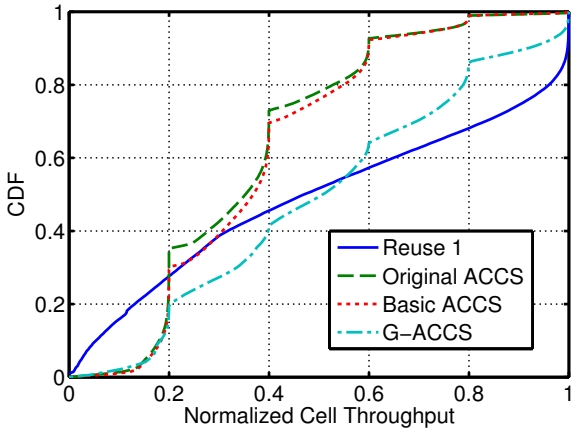

(b)

Fig. 5. Empirical cumulative distributions functions of normalized downlink cell throughput: (a) $\delta = 0.2$, $\lambda = 0.1$ and (b) $\delta = 0.8$, $\lambda = 0.1$. G-ACCS yields outage gains (lower tail) without sacrificing the performance along the rest of the distribution.

Additionally, once a cell activates a low quality SCC, it might be preventing its usage by other cells where it could be utilized in a more spectrally efficient manner. There are a few tactics to minimize this issue, but none really solves it without additional parametrization or trade-offs. For example, restricting the CCs selectable as BCCs to e.g. {1,2,3} will pack BCCs more tightly and therefore increase the probability of cells finding available SCCs. However, this will worsen BCC interference conditions. Alternatively, cells could adjust their respective C/I requirements according to the traffic load. Yet this implies extra signaling, and the dynamics of packet-switched traffic are not easily tracked, notably when signaling delays are involved.

G-ACCS greatly reduces the overprotection problem as shown in Fig. 5. In fact, its greatest merit is to achieve this goal without additional parameters and minimal sacrifice of fairness. It can be seen that the performance boost in the lower portion of the throughput distribution is maintained.

C. Analysis

This section condenses the results obtained and attempts to put them into perspective. Table II presents a summary of the performance of all considered component carrier selection strategies. The results are also plotted in Figs. 6a and 6b for $\delta = 0.2$ and $\delta = 0.8$, respectively. Each circle corresponds to a different λ, hence one session arriving on average every 10s, 5s and 1s after the end of the previous one. The points near the upper-right corner correspond to the lower lambda values. The x-axis is the average cell throughput, while the y-axis corresponds to the 5% outage user throughput. The diameter of the circles represents the peak user throughput with the actual values shown next to it for clarity. Finally, the dashed lines are polynomial trend lines.

TABLE II
SUMMARY OF SIMULATION RESULTS.

Deployment Ratio		$\delta = 0.2$			$\delta = 0.8$		
$E[\mathcal{I}]$	Scheme	Out	Avg	Peak	Out	Avg	Peak
$1/\lambda$=10s	R1	14%	86%	100%	2.4%	51%	100%
$1/\lambda$= 5s		9%	78%	100%	1.5%	35%	96%
$1/\lambda$= 1s		5%	60%	100%	0.9%	21%	64%
$1/\lambda$=10s	NLM	32%	55%	60%	4%	38%	60%
$1/\lambda$= 5s		31%	55%	60%	2.5%	30%	58%
$1/\lambda$= 1s		14%	49%	60%	1.7%	23%	50%
$1/\lambda$=10s	ACCS	20%	71%	100%	16%	37%	74%
$1/\lambda$= 5s		20%	69%	100%	14%	34%	69%
$1/\lambda$= 1s		19%	66%	100%	12%	30%	59%
$1/\lambda$=10s	G-ACCS	20%	86%	100%	16%	52%	100%
$1/\lambda$= 5s		19%	77%	100%	10%	41%	89%
$1/\lambda$= 1s		17%	70%	100%	6%	32%	72%

Analyzing Fig. 6 it is natural to ask which strategy is the best. True to the engineering spirit, the answer is: it depends. Universal reuse is a competitive solution in terms of simplicity, peak date rates and average cell throughput. Nevertheless, its outage performance, especially in denser deployments, is deplorable even at modest traffic loads. Therefore an operator opting for this strategy could face a throng of dissatisfied users. A situation that would be aggravated in case of heterogeneous co-channel deployments, since standardized schemes typically favor macro UEs at the expense of femto users [13].

One potential advantage of the NLM scheme is the absence of inter-cell signaling. Notwithstanding, its decent outage performance, particularly in less dense deployments, the NLM strategy suffers a major degradation in terms of peak data rates and overall cell capacity. Moreover, NLM displayed very poor outage performance in denser deployments, barely outperforming universal reuse. The results are nowhere near those achieved by the genie-aided reuse 1/2 pattern of previous contributions [38]. One of the reasons is the random (spatial) order in which femtocells are switched on. Without reconfigurations, the achieved CC pattern is far from optimal due to deadlocks. The overall performance results from NLM would certainly vary if the cardinality and number of the subsets were chosen differently. Yet, that would not change the fact that the method relies on measurements performed at transmitter side rather than the receiver side. The "nearest" neighbor as seen

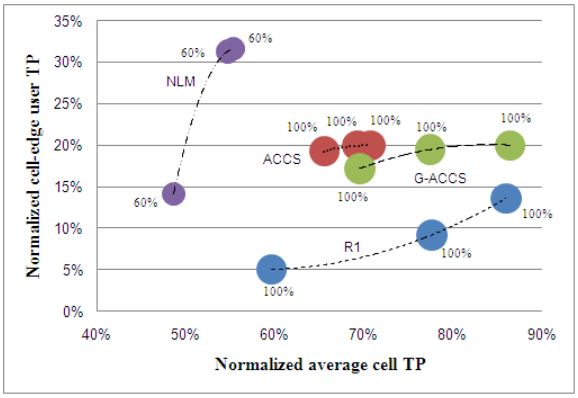

(a)

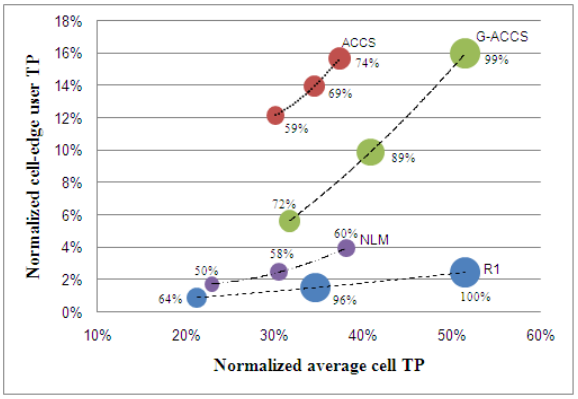

(b)

Fig. 6. Summary of attained performance for all considered component carrier selection strategies: (a) $\delta = 0.2$ and (b) $\delta = 0.8$. The bigger the "bubble" and the closer it is to the uppermost right corner the better. The numbers next to each bubble the percentage of the maximum throughput achieved by the best 5% users. The lines connecting the dots simply highlight the trends.

by the femtocell is not necessarily the strongest DL interferer. Furthermore, NLM-like methods overlook one critical trait of the spectrum sharing problem, as the amount of CCs is fixed. Discovering not only which, but also how many CCs should be allocated at a given time is equally, if not more, important.

The basic ACCS offers considerable performance improvements compared to the two aforementioned simpler techniques. Additionally, with five CCs to choose from, ACCS was found to be quite insensitive to the order in which femtocells are switched on. Current results and those reported in [14] indicate that the interference coupling expressed by BIMs successfully captures the spatial sparseness of the network. However the same cannot be said about the temporal sparseness. The outcome is a visible degradation in the average cell throughput and a more subtle loss in peak performance when compared with universal reuse. The trade-off is not deterministic and can be controlled by adjusting the C/I targets employed [14]. However, fine-tuning such targets is laborious, and the values tend to be case specific. In our studies we have used values optimized for full-buffer traffic, hence the excellent performance at high duty cycles and dense deployments.

G-ACCS is clearly the most well-rounded method. It retains

TABLE III
QUANTIFYING THE JOINT PERFORMANCE IN TERMS OF EFFICIENCY AND FAIRNESS.

Cases	δ	λ	R1	NLM	ACCS	G-ACCS
Joint Performance $(\mathcal{J}_{\text{scheme}} \times \mu^{\text{cell}}_{\text{scheme}})$	0.2	0.1	0.788	0.529	0.635	0.794
		0.2	0.673	0.530	0.611	0.680
		1	0.456	0.448	0.575	0.597
	0.8	0.1	0.354	0.306	0.307	0.415
		0.2	0.206	0.224	0.274	0.304
		1	0.114	0.160	0.241	0.226

the best aspects of ACCS and always outperforms universal reuse in terms of average cell-throughput, while attaining comparable peak data rates. An intuitive explanation comes from the model introduced in Section II-B. Since G-ACCS does not require hard decisions, it is capable of moving along the resource utilization plane seeking the best compromise. The rationale is a generalization of the temporal activity ratio concept to a resource utilization ratio. The latter is justified by the fact that transmit power is also a key resource in wireless networks.

Moreover, because fairness is an important aspect when multiple autonomous agents share a limited set of resources; we employ Jain's fairness index $(\mathcal{J})$ to quantify it. Jain's index is a continuous and scale-independent metric. It can be understood as the square of the cosine of the angle between the data set x_i and the hypothetical equal allocation and is defined as [45]:

$$\mathcal{J}(x_1, x_2, \ldots, x_n) = \frac{(\sum_{i=1}^{n} x_i)^2}{n \cdot \sum_{i=1}^{n} x_i^2} \tag{10}$$

A value of $\mathcal{J} = 1$ implies that all femtocells in the network achieve the same average DL throughput. Nonetheless, the fairness index per se says nothing about the absolute throughput attained by cells. It simply expresses the degree of equality. On the other hand, the average cell throughput (μ^{cell}) is a metric that masks inequality. Since we have two bounded metrics between 0 and 1, a natural development is to multiply both metrics $(\mathcal{J}_{\text{scheme}} \times \mu^{\text{cell}}_{\text{scheme}})$ in order to quantify the joint performance in terms of efficiency and fairness[4]. Table III summarizes this product for the different CC selection strategies under different traffic loads and density of femtocells.

Readers can verify that G-ACCS is exceptionally well positioned when fairness and performance metrics are combined. ACCS does outperform G-ACCS in the densest and most heavily loaded scenario, but this is a consequence of (i) the fine-tuned parametrization employed in ACCS and (ii) the pessimistic signaling delay assumptions which penalize G-ACCS more severely than ACCS due to the more permissive nature of the former.

Finally, we can state that our results make it very evident that both the spatial distribution of devices and temporal traits

[4]Strictly speaking, the lower bound of $\mathcal{J}$ equals $1/n$, which tends to 0 as n tends to infinity.

of traffic (from light loads to near full-buffer) are elements that should not be overlooked when designing solutions for future femtocells. It is rather straightforward to protect the less-favored users; any sparse static reuse pattern will do it. However doing so without compromising average and peak user throughput values under a multitude of unpredictably varying conditions is rather tricky. Yet G-ACCS achieves this goal.

VI. Conclusion

In this paper we have explored the possibilities offered by carrier aggregation (CA) in terms of interference management in the context of future LTE-Advanced femtocells. Both simple and more complex alternatives were considered. The ultimate goal was to assess how much complexity is required to provide efficient interference coordination on a component carrier level. The contribution is valuable as it provides guidelines for future deployments of femtocells. Moreover we provide a comprehensive characterization of the performance as a function of the network density and the traffic intensity. While the majority of previous contributions focus on the full-buffer model; we have considered a finite-buffer traffic model. The latter introduces rapid fluctuations of the interference levels, and therefore challenges the working assumptions of many techniques where the need for iterative reconfigurations is incautiously deemed a minor nuisance. The analysis of our simulation results shows that all considered component carrier selection strategies have their pros and cons. Nonetheless, the main contribution of this paper, namely G-ACCS, retains the best elements of the other alternatives providing gains in terms of outage, average cell and peak throughput without any parametrization. Finally, our findings are also applicable to femtocells without CA support. For example, if femtocells are restrained to a single component carrier, a savvy (re-)selection of BCCs is desirable. The information from BIMs could be utilized to strike a balance between the minimization of the outgoing interference and the usefulness of the new BCC; thus minimizing the chances of propagating a wave of reselections arbitrarily far inside the local cluster of femtocells. Investigation of the aforementioned ideas, the extension to scenarios with picocells, as well as characterizing the impact of mobility on BIMs in terms of inter-cell signaling are the subject of ongoing work.

References

[1] V. Chandrasekhar, J. Andrews, and A. Gatherer, "Femtocell networks: a survey," *Communications Magazine, IEEE*, vol. 46, no. 9, pp. 59–67, 2008.

[2] H. Claussen, "Performance of macro- and co-channel femtocells in a hierarchical cell structure," in *Personal, Indoor and Mobile Radio Communications, 2007. PIMRC 2007. IEEE 18th International Symposium on*, 2007, pp. 1–5.

[3] D. Lopez-Perez, A. Valcarce, G. De La Roche, E. Liu, and J. Zhang, "Access methods to wimax femtocells: A downlink system-level case study," in *Communication Systems, 2008. ICCS 2008. 11th IEEE Singapore International Conference on*, 2008, pp. 1657–1662.

[4] D. Lopez-Perez, A. Valcarce, G. de la Roche, and J. Zhang, "Ofdma femtocells: A roadmap on interference avoidance," *Communications Magazine, IEEE*, vol. 47, no. 9, pp. 41–48, 2009.

[5] Z. Bharucha, H. Haas, A. Saul, and G. Auer, "Throughput enhancement through femto-cell deployment," *European Transactions on Telecommunications*, vol. 21, no. 5, pp. 469–477, 2010. [Online]. Available: http://dx.doi.org/10.1002/ett.1428

[6] M. A. Ergin, K. Ramachandran, and M. Gruteser, "An experimental study of inter-cell interference effects on system performance in unplanned wireless lan deployments," *Computer Networks*, vol. 52, pp. 2728–2744, October 2008. [Online]. Available: http://portal.acm.org/citation.cfm?id=1410487.1410878

[7] G. Boudreau, J. Panicker, N. Guo, R. Chang, N. Wang, and S. Vrzic, "Interference coordination and cancellation for 4g networks," *Communications Magazine, IEEE*, vol. 47, no. 4, pp. 74–81, 2009.

[8] H. Holma and A. Toskala, *LTE for UMTS Evolution to LTE-Advanced*, 2nd ed. John Wiley & Sons, 2011.

[9] P. Mogensen, T. Koivisto, K. Pedersen, I. Kovacs, B. Raaf, K. Pajukoski, and M. Rinne, "Lte-advanced: The path towards gigabit/s in wireless mobile communications," in *Wireless Communication, Vehicular Technology, Information Theory and Aerospace Electronic Systems Technology, 2009. Wireless VITAE 2009. 1st International Conference on*, May 2009, pp. 147–151.

[10] S. Parkvall, A. Furuskar, and E. Dahlman, "Evolution of lte toward imt-advanced," *Communications Magazine, IEEE*, vol. 49, no. 2, pp. 84–91, 2011.

[11] K. Pedersen, F. Frederiksen, C. Rosa, H. Nguyen, L. Garcia, and Y. Wang, "Carrier aggregation for lte-advanced: functionality and performance aspects," *Communications Magazine, IEEE*, vol. 49, no. 6, pp. 89 –95, june 2011.

[12] M. Iwamura, K. Etemad, M.-H. Fong, R. Nory, and R. Love, "Carrier aggregation framework in 3GPP LTE-Advanced [WiMAX/LTE Update]," *Communications Magazine, IEEE*, vol. 48, no. 8, pp. 60–67, 2010.

[13] D. Lopez-Perez, I. Guvenc, G. de la Roche, M. Kountouris, T. Quek, and J. Zhang, "Enhanced intercell interference coordination challenges in heterogeneous networks," *Wireless Communications, IEEE*, vol. 18, no. 3, pp. 22–30, june 2011.

[14] L. Garcia, K. Pedersen, and P. Mogensen, "Autonomous component carrier selection: interference management in local area environments for lte-advanced," *Communications Magazine, IEEE*, vol. 47, no. 9, pp. 110–116, 2009.

[15] 3GPP, "Evolved Universal Terrestrial Radio Access (E-UTRA); FDD Home eNode B (HeNB) Radio Frequency (RF) requirements analysis," Tech. Rep., April.

[16] N. Devroye, M. Vu, and V. Tarokh, "Cognitive radio networks," *Signal Processing Magazine, IEEE*, vol. 25, no. 6, pp. 12–23, 2008.

[17] L. Narayanan, *Channel Assignment and Graph Multicoloring*. John Wiley & Sons, Inc., 2002, pp. 71–94.

[18] M. C. Necker, "Scheduling Constraints and Interference Graph Properties for Graph-based Interference Coordination in Cellular OFDMA Networks," *Mob. Netw. Appl.*, vol. 14, pp. 539–550, August 2009. [Online]. Available: http://dx.doi.org/10.1007/s11036-009-0155-8

[19] Furqan Ahmed and Olav Tirkkonen and Matti Peltomäki and Juha-Matti Koljonen and Chia-Hao Yu and Mikko Alava, "Distributed Graph Coloring for Self-Organization in LTE Networks," *Journal of Electrical and Computer Engineering*, vol. 2010, August 2010.

[20] Michael Garey and David S. Johnson, *Computers and Intractability: A Guide to the Theory of NP-Completeness*. W. H. Freeman, 1979.

[21] M. Huson and A. Sen, "Broadcast scheduling algorithms for radio networks," in *Military Communications Conference, 1995. MILCOM '95, Conference Record, IEEE*, vol. 2, Nov. 1995, pp. 647–651 vol.2.

[22] A. Mishra, S. Banerjee, and W. Arbaugh, "Weighted coloring based channel assignment for wlans," *SIGMOBILE Mob. Comput. Commun. Rev.*, vol. 9, pp. 19–31, July 2005. [Online]. Available: http://doi.acm.org/10.1145/1094549.1094554

[23] D. Leith and P. Clifford, "A self-managed distributed channel selection algorithm for wlans," in *Modeling and Optimization in Mobile, Ad Hoc and Wireless Networks, 2006 4th International Symposium on*, 2006, pp. 1–9.

[24] I. Katzela and M. Naghshineh, "Channel assignment schemes for cellular mobile telecommunication systems: A comprehensive survey," *Communications Surveys Tutorials, IEEE*, vol. 3, no. 2, pp. 10–31, 2000.

[25] M.-L. Cheng and J.-I. Chuang, "Performance evaluation of distributed measurement-based dynamic channel assignment in local wireless communications," *Selected Areas in Communications, IEEE Journal on*, vol. 14, no. 4, pp. 698–710, May 1996.

[26] M. Serizawa and D. Goodman, "Instability and deadlock of distributed dynamic channel allocation," in *Vehicular Technology Conference, 1993 IEEE 43rd*, May 1993, pp. 528–531.

[27] Jeffrey G. Andrews and Wan Choi and Robert W. Heath Jr, "Overcoming Interference in Spatial Multiplexing MIMO Cellular Networks," *Wireless Communications Magazine, IEEE* , December 2007.
[28] A. MacKenzie and S. Wicker, "Game theory and the design of self-configuring, adaptive wireless networks," *Communications Magazine, IEEE*, vol. 39, no. 11, pp. 126–131, Nov. 2001.
[29] J. Ellenbeck, C. Hartmann, and L. Berlemann, "Decentralized inter-cell interference coordination by autonomous spectral reuse decisions," in *Wireless Conference, 2008. EW 2008. 14th European*, 2008, pp. 1–7.
[30] G. da Costa, A. Cattoni, I. Kovacs, and P. Mogensen, "A scalable spectrum-sharing mechanism for local area network deployment," *Vehicular Technology, IEEE Transactions on*, vol. 59, no. 4, pp. 1630–1645, May 2010.
[31] I. Akyildiz, W.-Y. Lee, M. Vuran, and S. Mohanty, "A survey on spectrum management in cognitive radio networks," *Communications Magazine, IEEE*, vol. 46, no. 4, pp. 40–48, 2008.
[32] A. Galindo-Serrano, L. Giupponi, and M. Dohler, "Cognition and Docition in OFDMA-Based Femtocell Networks," in *GLOBECOM 2010, 2010 IEEE Global Telecommunications Conference*, dec. 2010, pp. 1–6.
[33] M. Haenggi, J. Andrews, F. Baccelli, O. Dousse, and M. Franceschetti, "Stochastic geometry and random graphs for the analysis and design of wireless networks," *Selected Areas in Communications, IEEE Journal on*, vol. 27, no. 7, pp. 1029–1046, 2009.
[34] 3GPP, "Evolved Universal Terrestrial Radio Access (E-UTRA); Physical layer; Measurements," Tech. Spec. 36.214 V10.1.0, March 2011. [Online]. Available: http://www.3gpp.org
[35] P. Mogensen, W. Na, I. Kovacs, F. Frederiksen, A. Pokhariyal, K. Pedersen, T. Kolding, K. Hugl, and M. Kuusela, "LTE Capacity Compared to the Shannon Bound," in *Vehicular Technology Conference*, April 2007, pp. 1234–1238.
[36] C. Shannon, "A Mathematical Theory of Communication," *the Bell System Technical Journal*, 1948.
[37] A. Simonsson, "Frequency reuse and intercell interference co-ordination in e-utra," in *Vehicular Technology Conference, 2007. VTC2007-Spring. IEEE 65th*, 2007, pp. 3091–3095.
[38] Y. Wang, S. Kumar, L. Garcia, K. Pedersen, I. Kovacs, S. Frattasi, N. Marchetti, and P. Mogensen, "Fixed frequency reuse for lte-advanced systems in local area scenarios," in *Vehicular Technology Conference, 2009. VTC Spring 2009. IEEE 69th*, 2009, pp. 1–5.
[39] J. Zhang and G. de la Roche, *Femtocells: Technologies and Deployment*. John Wiley and Sons, 2010, ch. 8.5, pp. 234–235.
[40] L. Garcia, K. Pedersen, and P. Mogensen, "Autonomous component carrier selection for local area uncoordinated deployment of lte-advanced," in *Vehicular Technology Conference Fall (VTC 2009-Fall), 2009 IEEE 70th*, 2009, pp. 1–5.
[41] F. Sanchez-Moya, J. Villalba-Espinosa, L. G. U. Garcia, K. I. Pedersen, and P. E. Mogensen, "On the Impact of Explicit Uplink Information on Autonomous Component Carrier Selection for LTE-A Femtocells," in *Vehicular Technology Conference Spring (VTC 2011-Spring), 2010 IEEE 72nd*, 2010, pp. 1–5.
[42] L. Zhang, L. Yang, and T. Yang, "Cognitive Interference Management for LTE-A Femtocells with Distributed Carrier Selection," in *Vehicular Technology Conference Fall (VTC 2010-Fall), 2010 IEEE 72nd*, 2010, pp. 1–5.
[43] 3GPP, "Physical layer aspects for evolved Universal Terrestrial Radio Access (UTRA)," Tech. Rep. 25.814 v7.1.0, September 2006.
[44] 3GPP , "Evolved Universal Terrestrial Radio Access (E-UTRA); Further advancements for E-UTRA physical layer aspects," Tech. Rep. 36.814 v9.0.0, March 2010.
[45] J.-Y. Le Boudec, *Performance Evaluation of Computer and Communication Systems*. EPFL Press, Lausanne, Switzerland, 2010.

Luis Guilherme Uzeda Garcia received his 5 year diploma in Electronics and Computer Engineering from the Federal University of Rio de Janeiro (UFRJ) in 2003 and his M.Sc.E.E. degree from COPPE/UFRJ, Brazil, in 2006. He also worked as a researcher at Instituto Nokia de Tecnologia (INdT) in Brasília, Brazil, for four years. He is currently concluding his Ph.D. research at Aalborg University, Denmark, in close cooperation with Nokia Siemens Networks. His current work is related to dynamic spectrum sharing, femtocells, distributed systems, 3GPP standardization of LTE-Advanced, and future radio access technologies.

István Zsolt Kovács has received his B.Sc. from "Politehnica" Technical University of Timişoara, Romania in 1989, his M.Sc.E.E. from The Franco-Polish School of New Information and Communication Technologies/Ecole Nationale Supérieure des Télécommunications de Bretagne, Poland/France in 1996, and his Ph.D.E.E. in Wireless Communications from Aalborg University, Denmark in 2002. From 2002 to August 2005 he held the position of assistant research professor with Center For TeleInFrastruktur, Department of Communication Technology of Aalborg University, in the Antennas and Propagation division. Currently István Z. Kovács has the position of Wireless Networks Specialist in Nokia Siemens Networks, Aalborg, Denmark, where he conducts research on radio capacity analysis and broadband traffic evolution in HSPA and LTE/LTE-A network deployments.

Klaus Ingemann Pedersen received his M.Sc. E.E. and Ph.D. degrees in 1996 and 2000 from Aalborg University, Denmark. He is currently with Nokia Siemens Networks in Aalborg, Denmark, where he is working as a senior wireless network specialist. His current work is related to 3GPP standardization of Long Term Evolution (LTE) Advanced. The latter includes work on interference management, mobility, and performance of heterogeneous networks with mixture of different base station types.

Gustavo Wagner Oliveira da Costa has received his Electrical Engineer degree and M.Sc.E.E. from the University of Brasília, Brazil, in 2004 and 2008, respectively. From 2005 until 2007 he worked as a research engineer at Instituto Nokia de Tecnologia (INdT) in Brasília, Brazil. He is currently working toward a Ph.D. degree at Aalborg University, Denmark, in close cooperation with Nokia Siemens Networks. His current research interests include dynamic spectrum sharing, femtocells, radio resource management and concept development for IMT-Advanced systems.

Preben Elgaard Mogensen received his M.Sc. E.E. and Ph.D. degrees in 1988 and 1996 from Aalborg University, Denmark. He is currently Professor at Aalborg University leading the Ratio Access Technology Section. Preben Mogensen is also part time associated with Nokia Siemens Networks. His current research work is related to heterogenous networks deployment, cognitive radio and beyond 4G.